Available online at www.sciencedirect.com
ScienceDirect
C. R. Mecanique 337 (2009) 131–140
COMPTES RENDUS MECANIQUE

Modeling and identification of a solenoid valve for PWM control applications

M. Taghizadeh [a,b,*], A. Ghaffari [a], F. Najafi [a]

[a] *Mechanical Eng. Department, K.N. Toosi University of Technology, Tehran, PO Box 15875-4416, Iran*
[b] *Control Engineering Department, Power and Water University of Technology (PWUT), Tehran, PO Box 16765-1719, Iran*

Received 21 January 2009; accepted after revision 18 March 2009

Available online 11 April 2009

Presented by Jean-Baptiste Leblond

Abstract

In this Note, a nonlinear dynamic model of a PWM-driven pneumatic fast switching valve is presented. The electro-magnetic, mechanical and fluid subsystems of the valve are investigated, including their interactions. Unknown parameters are identified using direct search optimization and model validation is performed by comparing the simulated and measured current curves. In order to use this model in PWM control applications, a simplification strategy is also proposed and a static model is obtained between the duty cycle input and the moving average of the spool position. The simplified static model is validated again by experiments. ***To cite this article: M. Taghizadeh et al., C. R. Mecanique 337 (2009).***

Keywords: Fluid mechanics; Modeling; Identification; Solenoid valve; PWM; Servo-pneumatic; Simulation

1. Introduction

Electro-pneumatic control valves are used as interfaces between electronic controls and fluid flow. There are two types of electro-pneumatic valves to control the fluid flow of a pneumatic actuator. These are the continuously acting servo/proportional valves and the on–off switching valves. Due to having proportional input–output behavior, pneumatic servo systems are usually realized by the continuously acting servo/proportional valves. But these valves have complex structures, are very costly and tend to be bulky compared to inexpensive, compact and lightweight switching valves. Therefore, servo-pneumatic systems utilizing fast switching valves have been developed [1–3].

In order to use the discrete on–off switching valves instead of the continuously acting servo valves and to obtain similar proportional characteristics, pulse width modulation (PWM) techniques are used. Applying the PWM signal as the control input to a switching valve makes the valve on and off successively. As a result, fluid is passed through a valve that is completely open or completely closed and is delivered to the actuator as discrete packets of mass.

* Corresponding author.
E-mail address: taghizadeh@pwut.ac.ir (M. Taghizadeh).

1631-0721/$ – see front matter
doi:10.1016/j.crme.2009.03.009

Bigger pulse widths result in bigger packets of fluid. If the time rate of delivery of these packets (PWM frequency) is considerably faster than the dynamics of the actuator and load, then the system filters the discreteness of the packets and responds to the average of the input signal, similar to the continuous case [4].

PWM-driven fast switching valves are employed in several areas of industrial applications. A typical application of this kind for pneumatic systems is the realization of control functions in intelligent electro-pneumatic braking systems of motor vehicles [5]. Many other pneumatic servo control applications in robotics [6–8] and other areas [9–11] have been pursued by researchers in order to reduce the cost, complexity and weight of the system by utilizing switching valves instead of servo valves. These techniques have been also successfully applied to hydraulic servo systems [12,13]. The fully variable valve actuation in combustion engines can be mentioned as an application of PWM-driven hydraulic switching valves which improves the performance and efficiency of the engine [14].

Dynamic characteristics of fast switching solenoid valves influence the successful operation of the entire fluid power system. Therefore, it is of critical importance to elaborate a reliable dynamical model for these valves to be applied in design of the fluid power hardware and its control. The model must accurately handle the three constituting subsystems of the valve, namely the electromagnetic, mechanical and fluid subsystems.

There are many works in which the modeling and control of pneumatic actuators are considered [15–20]. However, very few authors have treated the modeling of solenoid valves. Ye et al. [21] investigated some static characteristics of a PWM solenoid valve and presented an equation for determining the maximum operating modulation ratio. Sethson et al. [14] proposed a simple model for a 2/2 hydraulic solenoid valve in which the model parameters are tuned to yield good agreement between the measured and the simulated variables. Yuksel et al. [22] designed a new pneumatic solenoid valve and investigated its dynamic model to describe the switching characteristics of the valve. Other investigations into the behavior of pneumatic fast switching valves can be found in [23,24]. In the above works, solenoid valves are studied from the viewpoint of valve design. However, the main objective of the present modeling is to emphasize on the applicability of the model in the controller design process for PWM-driven servo-pneumatic systems.

In this Note, modeling and identification of a PWM-driven pneumatic fast switching valve are presented. In the following, in Section 2, the internal structure of the valve is investigated and the electro-magnetic, mechanical and fluid subsystems are discussed including their interactions. In Section 3, governing equations of the valve are derived in the form of nonlinear state equations. In Section 4, identification of the unknown parameters and validation of the model are performed by comparing the simulated and measured currents of the solenoid. The nonlinear dynamical model obtained so far is a powerful simulation and computational tool; however it should be simplified in order to be effectively used in control design applications. This task is performed in Section 5 in which the moving average of the spool position is calculated and a simplified static model is presented between the duty cycle of the PWM input and the averaged spool position. Finally, Section 6 contains some concluding results.

2. Structure of the valve

The solenoid valve under study is a fast switching spring return 3/2 valve. In Fig. 1, simplified schematic views are shown to indicate the closed and open positions of the valve. In the absence of solenoid excitation, the valve is kept at its closed end-position by the return spring (Fig. 1(a)). When the solenoid is energized by DC voltage, the resultant magnetic force displaces the moving part against the return spring, valve opens (Fig. 1(b)) and a flow cross section develops through an orifice.

A block diagram representation of the valve is given in Fig. 2 which indicates the signal flow of the model from the input voltage to the output flow, including the intermediate interactions. As shown in this figure, a solenoid valve can be decomposed into three interacting subsystems; the electromagnetic, mechanical and fluid subsystems.

The two first subsystems, namely the solenoid with its electromagnetic equations, and the mechanical part consisting of a mass–spring–damper system, behave dynamically and have transient responses. In the next section, the nonlinear dynamic equations governing these subsystems will be derived in which the pressure forces are also included. The third subsystem, namely the valve orifice, can be described by the general orifice equation for turbulent flow [22].

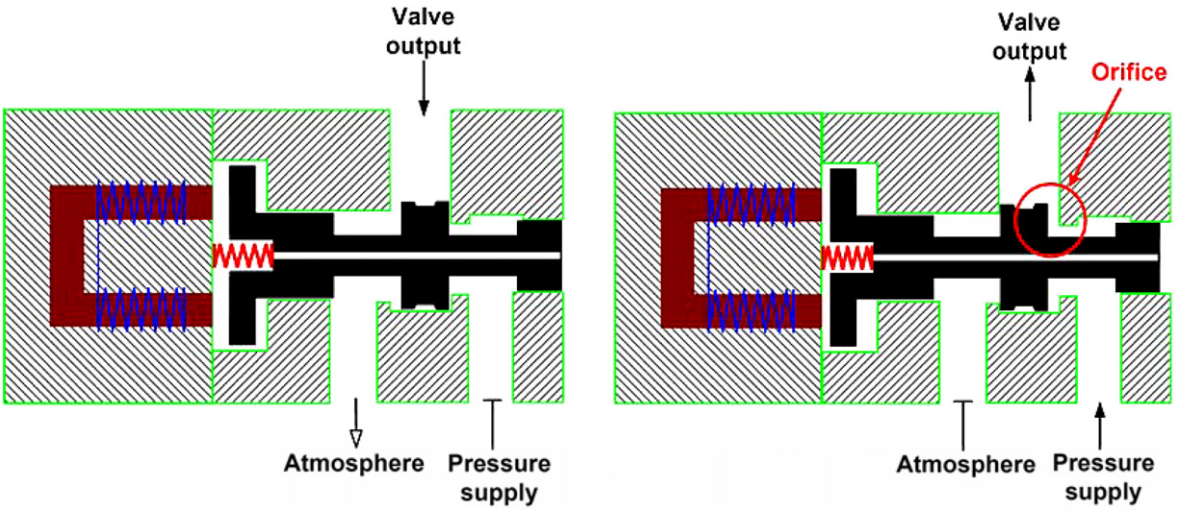

Fig. 1. Schematic of the valve operation. (a): closed, (b): open.

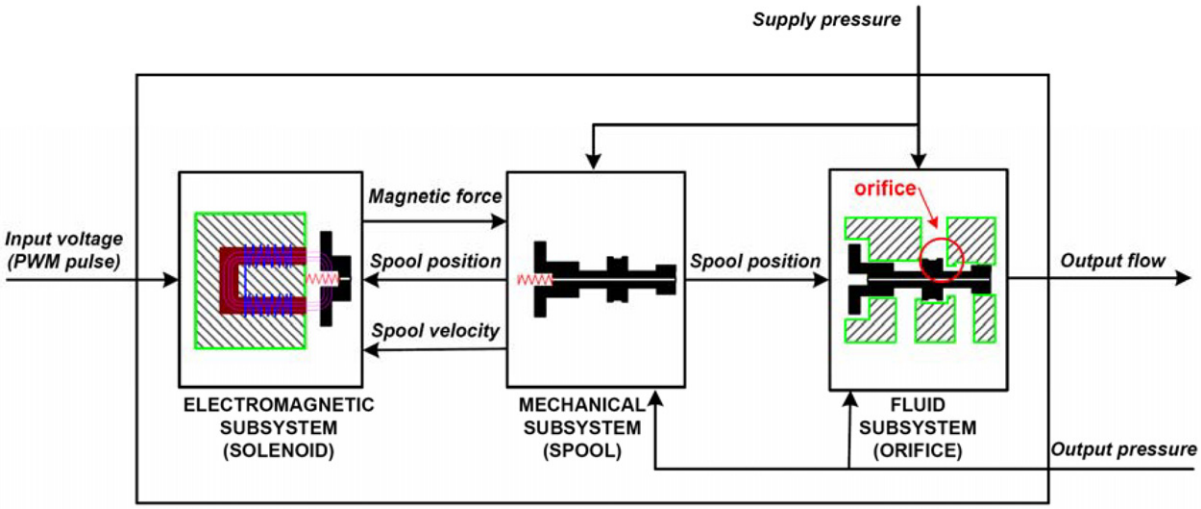

Fig. 2. Block diagram representation of the valve subsystems and their interactions.

3. Valve modeling

A solenoid valve is a complex technical system whose characteristic is governed by a couple of interacting electro-magnetic, mechanical and flow equations. In the following, different subsystems of a solenoid valve are investigated and the governing equations are derived in the form of nonlinear state equations. For this purpose, the solenoid current $i(t)$, the spool position $x(t)$, and the spool velocity $\dot{x}(t)$ are selected as state variables. It is tried to derive a simple, yet accurate model, with a reasonable number of parameters, so that it can be used as an effective simulation tool.

3.1. Electromagnetic subsystem

This subsystem consists of an electrical and magnetic circuit included in a solenoid. The solenoid model has to handle the transformation of the input voltage to an electro-magnetic force on the spool of the valve. The electrical circuit is the actual coil which is represented with a variable inductance L in series with a resistance R of the coil.

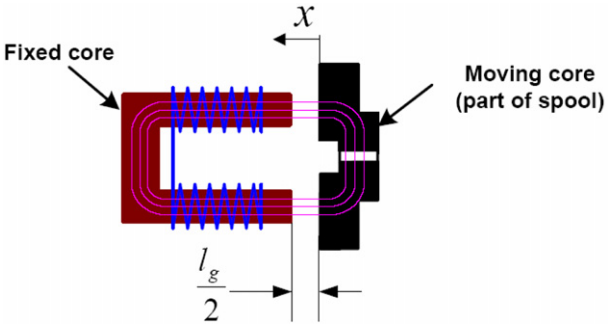

Fig. 3. Schematic of the magnetic circuit.

The magnetic circuit consists of a fixed core surrounded by the coil turns, and a moving part which is connected to the spool and moves with the spool under the effect of the exerted magnetic force. The magnetic circuit is schematically shown in Fig. 3. For this circuit, the electromotive force can be stated as

$$Ni = H_c l_c + H_g l_g = H_c l_{eq} \tag{1}$$

where N is the number of coil turns, and H_c and H_g are the magnetic field intensity in the core and in the air gap respectively. Parameters l_c and l_g are the length of magnetic circuit inside the core and in the air gaps and l_{eq} represents the equivalent length of the total magnetic circuit. It is assumed that the air gaps are small enough to ignore the fringing of the flux, therefore l_{eq} can be given by

$$l_{eq} = l_c + \frac{\mu_c}{\mu_0} l_g = l_c + 2\mu_r (x_t - x); \quad \mu_r = \frac{\mu_c}{\mu_0}, \quad l_g = 2(x_t - x) \tag{2}$$

in which μ_c and μ_0 are the permeability of the core and air, respectively, and μ_r is the relative permeability of the core. x_t is the total air gap including a traveling and a holding air gap. When the spool is in its initial position ($x = x_{\min}$), then l_g has its maximum value (total air gap), and as the spool comes to its maximum travel ($x = x_{\max}$), l_g has its minimum value (holding gap).

Using (1), together with the following fundamental relations:

$$\begin{cases} H_c = \frac{B}{\mu_c} = \frac{\varphi}{A_e \mu_c} \\ Li = N\varphi \end{cases} \tag{3}$$

the variable inductance of the magnetic circuit, $L(t)$, is given as a function of spool position

$$L(t) = \frac{N^2 A_e \mu_c}{l_{eq}} = \frac{N^2 A_e \mu_c}{l_c + 2\mu_r (x_t - x(t))} \tag{4}$$

where φ is the magnetic flux, B is the density of magnetic flux and A_e is the effective cross sectional area of flux path.

Now, the state equation of this subsystem can be written by applying Kirchhoff's voltage law

$$V(t) = Ri(t) + \frac{\mathrm{d}}{\mathrm{d}t} L(t) i(t) = Ri(t) + L(t) \frac{\mathrm{d}}{\mathrm{d}t} i(t) + i(t) \frac{\mathrm{d}}{\mathrm{d}t} L(t) \tag{5}$$

in which $V(t)$ is the input voltage and $i(t)$ is the electrical current. Differentiating $L(t)$ gives

$$\frac{\mathrm{d}}{\mathrm{d}t} L(t) = \frac{2\mu_r N^2 A_e \mu_c \dot{x}(t)}{[l_c + 2\mu_r (x_t - x(t))]^2} = \frac{2\mu_r L^2(t) \dot{x}(t)}{N^2 A_e \mu_c} \tag{6}$$

Substituting (6) into (5), we get the first nonlinear state equation as

$$\frac{\mathrm{d}}{\mathrm{d}t} i(t) = \frac{1}{L(t)} \big[V(t) - Ri(t) \big] - \frac{2\mu_r L(t) \dot{x}(t) i(t)}{N^2 A_e \mu_c} \tag{7}$$

Also, the magnetic attraction force of the solenoid can be stated as

$$F_m = 2 \frac{\varphi^2}{2 A_e \mu_0} = \frac{L(t)^2 i(t)^2}{N^2 A_e \mu_0} \tag{8}$$

In the next subsection, two other state equations representing x and $\dot{x}$ will be derived.

3.2. Mechanical subsystem

The mechanical subsystem consists of a mass, spring and damper under the effect of magnetic and pressure forces. It can be represented by Newton's second law as

$$m_s \frac{\mathrm{d}^2}{\mathrm{d}t^2} x(t) + b \frac{\mathrm{d}}{\mathrm{d}t} x(t) + k\big(x(t) + \delta\big) = F_m(t) + F_{prs} \tag{9}$$

in which m_s is the spool mass, b and k are the damping and spring coefficients, δ is the spring pre-tension and F_{prs} is the pressure force. The pressure force can be simply approximated by

$$F_{prs} = (A_1 - A_2) P_{\sup} + (A_3 - A_4) P_{out} \tag{10}$$

where $P_{\sup}$ and P_{out} are the pressures at the supply and output ports of the valve, and A_1, A_2, A_3 and A_4 are different areas on the spool lands which are affected by $P_{\sup}$ or P_{out} in different directions. In the valve studied, the areas A_3 and A_4 are approximately equal such that the effect of P_{out} on F_{prs} can be neglected.

Now, by selecting x and $\dot{x}$ as state variables and rewriting (9), the two other state equations are obtained as

$$\begin{cases} \dfrac{\mathrm{d}}{\mathrm{d}t} x(t) = \dot{x}(t) \\ \dfrac{\mathrm{d}}{\mathrm{d}t} \dot{x}(t) = \dfrac{1}{m_s}\big(-b\dot{x}(t) - k\big(x(t) + \delta\big) + F_m(t) + F_{prs}\big) \end{cases} \tag{11}$$

3.3. Fluid subsystem

The electromagnetic and mechanical parts of the valve are used to control the fluid flow through the valve orifice by controlling the spool position. The orifice equation for turbulent flow is used to describe the air flow through the valve [22]. This equation consists of two different static functions for subsonic and choked (sonic) flow regimes. As the fluid in the valve and in the pneumatic system is compressible, when the ratio of the upstream pressure ($P_{\sup}$) to the downstream pressure (P_{out}) is larger than a critical value, the flow regime is subsonic and the mass flow depends nonlinearly on both pressures. Whereas, when the pressure ratio is smaller than the critical ratio, the flow attains sonic velocity (choked flow) and depends linearly on the upstream pressure. In both cases, the air mass flow depends linearly on spool position. The standard equation for mass flow rate through an orifice is given by

$$\frac{\mathrm{d}m}{\mathrm{d}t} = \begin{cases} 0.0405 C_d . C_A . \bar{x}(t) \dfrac{P_{\sup}}{\sqrt{T}} & \text{if } \dfrac{P_{out}}{P_{\sup}} \leqslant 0.528 \\ C_d . C_A . \bar{x}(t) \dfrac{P_{\sup}}{\sqrt{T}} \left(\dfrac{2\gamma}{R(\gamma-1)} \left(\left(\dfrac{P_{out}}{P_{\sup}} \right)^{\frac{2}{\gamma}} - \left(\dfrac{P_{out}}{P_{\sup}} \right)^{\frac{\gamma+1}{\gamma}} \right) \right)^{1/2} & \text{if } \dfrac{P_{out}}{P_{\sup}} \geqslant 0.528 \end{cases} \tag{12}$$

where C_d is the discharge coefficient, C_A is the constant of the orifice cross sectional area, T is the supply temperature, R is the ideal gas constant and γ is the ratio of specific heats.

The controlling variable of the orifice in a PWM-driven valve is considered to be the average of the spool position denoted by $\bar{x}(t)$. In Section 5, calculation of $\bar{x}(t)$ from the simulated position of the spool, $x(t)$, will be discussed.

4. Parameter identification and model validation

Some of the model parameters are directly obtainable by measurement whereas some others are hard or impossible to measure, especially when it comes to magnetic material properties. The directly measured parameters and their values are listed in Table 1.

Table 1
The directly measured parameters.

Parameter	m_s	k	N	A_1	A_2	$A_3 = A_4$
Measured value	27 (gr)	10 000 (N/m)	1250	26.57 (mm^2)	35.25 (mm^2)	55.86 (mm^2)

Table 2
The identified parameters.

Parameter name	Measured value	Identified value	Parameter name	Measured value	Identified value
l_c	11 (cm)	11.5 (cm)	δ	1.1 (mm)	1.1 (mm)
R	15 (Ω)	13 (Ω)	x_t	0.35 (mm)	0.4 (mm)
$x_{\max}$	0.3 (mm)	0.33 (mm)	b	–	0.2 (N s/m)
A_e	0.75 (cm^2)	0.8 (cm^2)	μ_r	–	120

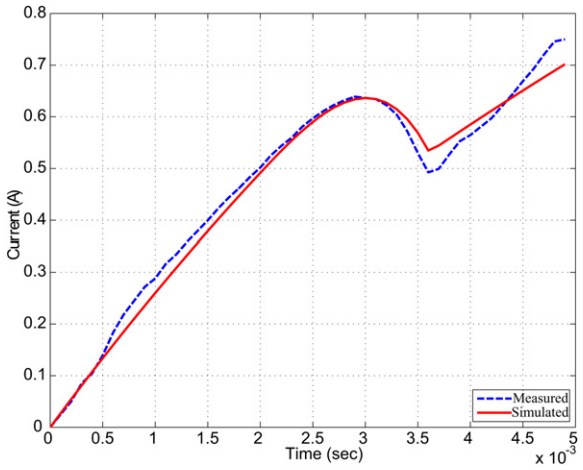

Fig. 4. Measured and simulated currents with a 24 volt input.

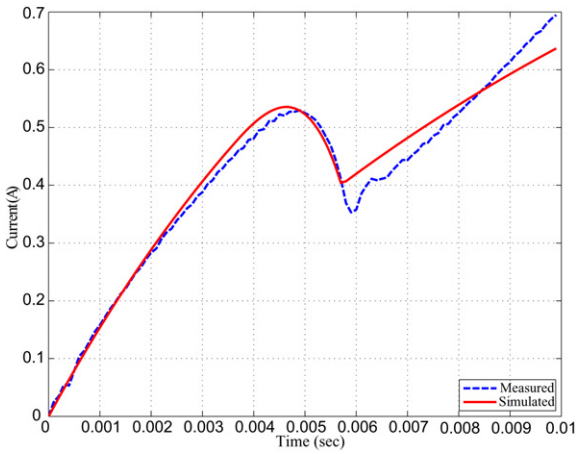

Fig. 5. Measured and simulated currents with a 15 volt input.

Direct measurement of some other parameters may seem to be possible; however, their real values may differ from the measurements due to several reasons. For example by measuring the geometrical dimensions of the core, the magnetic parameters A_e and l_c can be obtained. But they may have rather larger values than measurements. This is most likely due to the fact that a lumped parameter modeling of the magnetic circuit is performed which does not account for the exact geometrical shape. Another geometric parameter is x_t (the total length of air gap) which is very small and considerably affected by the measurement errors. The coil resistance is also measured for cold coil and should be tuned by an optimization strategy in order to account for the variations due to heating. There are also some unmeasured parameters like μ_r and b which are determined by identification.

In order to identify the unknown parameters, a direct search optimization method is applied which minimizes the integral of the absolute error between the simulated current of the model and the measured current of the actual solenoid. For this purpose, a physically sensible range of variation (based on the measurements) is selected for each unknown parameter and the equations of the mathematical model are solved numerically in MATLAB/SIMULINK environment.

Fig. 4 shows the measured current (with about 0.5% measurement error) of the actual solenoid together with the optimized simulated current. As indicated in this figure, good agreement is seen between the two curves which correspond to a set of identified parameters, listed in Table 2.

It should be noted that the current curves of Fig. 4 are obtained by applying a 24 volt input which is the standard working voltage of the solenoid valve. In order to validate the model and the identified parameters, another comparison is made between the measured and simulated currents by applying a 15 volt input. The results are shown in Fig. 5 which indicate proper agreement between the two curves and approve the validity of the model.

The time interval of the current in Fig. 4 consists of several stages which should be interpreted and justified with the actual behavior of the valve. These stages may be described as follows:

- The input voltage is applied at $t = 0$ and the current starts to rise until the magnetic force overcomes the spring force and the spool starts to move at approximately $t = 3$ ms;

- As a result of spool motion, the length of air gap decreases and the solenoid inductance increases (Eqs. (2) and (4)). Consequently, the current experiences a local peak (about 0.64 A) and begins to decrease until the spool reaches its end stroke and stops at approximately $t = 3.7$ ms (the complete opening time of the studied valve is 3.7 ms);
- When the spool stops, the inductance of the solenoid becomes constant and the current starts increasing again. As far as the input voltage is applied, the current continues to increase exponentially (the behavior of a first order R-L circuit) to reach a steady state value.

After the valve completely opens, the amount of current needed to keep the spool at its end position (holding current) is much less than the current needed for moving the spool from its initial position (switching current). On the other hand, the valve closing time is considerably dependant on the amount of current at the beginning of the de-energizing process.

In order to decrease the valve closing time, after the valve completely opens, current is reduced and remained at a constant holding level (about 0.5 A). In the actual valve, this task is performed by an internal electronic circuit which controls the current by converting the applied input voltage into a pulse width modulated voltage. It should be noted that, the valve itself is typically driven by PWM inputs, however the frequency of the internal PWM voltage (for controlling the current) should be higher enough than the frequency of the main input. In the simulation model, a separate PWM generator and a PI controller are designed to maintain the 0.5 A holding current. Another attempt for decreasing the closing time of the valve is to apply a negative voltage at the beginning of the de-energizing process. This task is realized by a capacitor which is charged during the valve opening and is used reversely during the valve closing. In the simulation model, this task is performed by a low-pass filter with initial value.

As an example, a 50 Hz PWM input with 40% duty cycle is applied and simulation results are shown in Fig. 6. Different stages of the applied voltage including the main PWM input, the re-modulated PWM signal (with higher frequency for controlling the holding current), and the negative voltage applied by the capacitor are noticeable in this figure. The controlled holding current and the opening and closing delay times of the valve are also recognizable from the current and spool position curves in the figure. These are all shown in one figure in order to indicate the correspondence between the voltage, current and spool position.

5. Model simplification

In this section, the obtained state space model is simplified in order to be practically applied in the design of servo-pneumatic control systems. From the viewpoint of control, in a PWM-driven valve, the average of the spool position can be considered as a control variable which meters the fluid flow through the valve orifice. Therefore, the average of the spool position in each PWM period (moving average) should be calculated and used instead of the spool

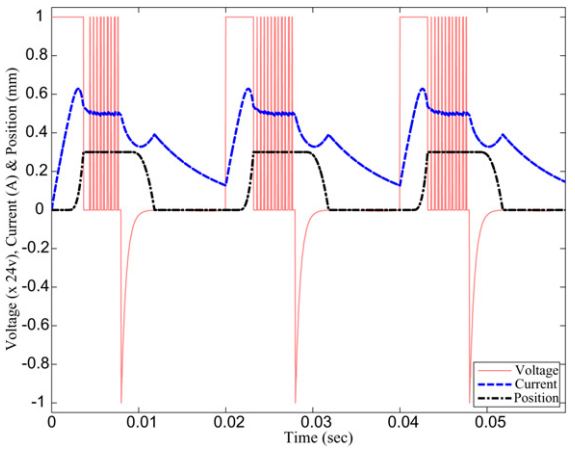

Fig. 6. Correspondence between the applied voltage, the current and the spool position.

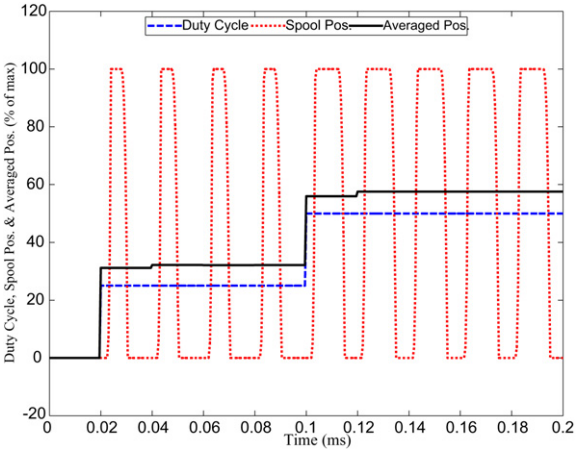

Fig. 7. Step change in the duty cycle, the spool position and its moving average.

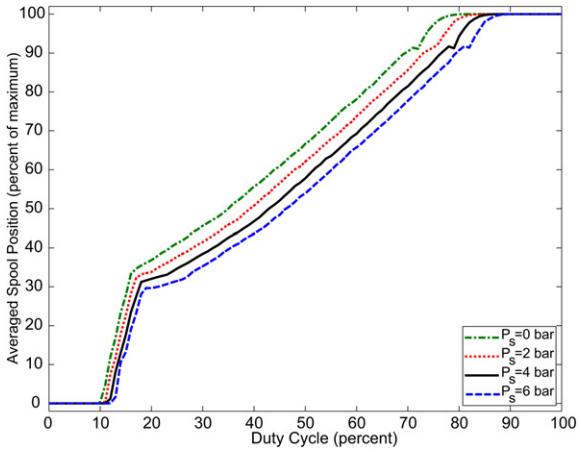

Fig. 8. Average spool position vs. duty cycle for $f_{\mathrm{PWM}} = 50$ Hz and different supply pressures.

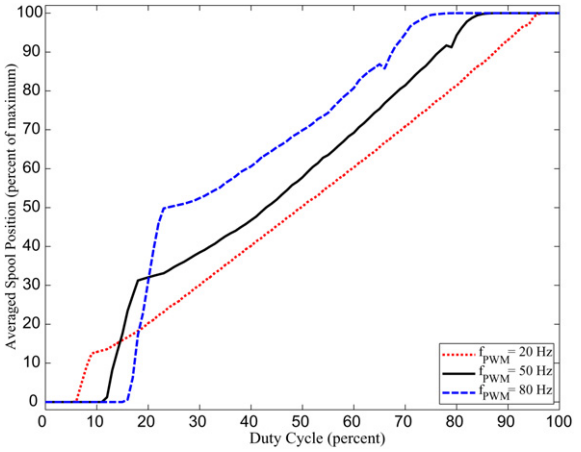

Fig. 9. Average spool position vs. duty cycle for $P_s = 4$ bar and different PWM frequencies.

position itself. For this purpose, the state space model is used as a computational tool to simulate the spool position and calculate its moving average. As an example, Fig. 7 shows the simulated spool position together with its average while a 50 Hz PWM input is applied and the duty cycle has changed from 25% to 50%.

As seen in Fig. 7, rapid transient behaviors (only in the first cycle after the step input change) are detectable in the response of the average spool position. For typical PWM control applications, these transient behaviors can be neglected in comparison with the dynamics of the other components of a servo-pneumatic system. Therefore, the valve model between the duty cycle input and the steady state values of the average spool position can be represented by a nonlinear static curve. This static model also depends on the frequency of the input pulse and the supply pressure. Fig. 8 indicates the average spool position (stated in percent of $x_{\max}$) vs. duty cycle, corresponding to a 50 Hz PWM frequency and different supply pressures. In Fig. 9, the effect of frequency is investigated by simulating the model in different frequencies and a constant pressure supply of 4 bar.

As seen in Fig. 8, increasing the supply pressure decreases the average of spool position. Referring to (10), since $(A_1 - A_2)$ is negative, the resultant force of P_{sup} is against the spool movement and decreases the average of spool position. In other words, it can be stated that P_{sup} shifts the effective range of duty cycle (full range excluding the dead band and the saturated region), without changing the size of this range. On the other hand, Fig. 9 indicates that increasing the PWM frequency decreases the effective range of duty cycle. Practically, in order to have a proper range of effective duty cycle, the PWM frequency should not be selected too high.

Finally, the static model is validated again by performing some experimental measurements. For this purpose, a 50 Hz PWM input is applied to the valve and the duty cycle is varied from 0% to 100%. A constant supply pressure of 4 bar is maintained and the steady state output flow of the valve is measured for any given duty cycle. Since flow is exhausted to atmosphere, the output pressure is small enough to assume a choked flow regime. According to (12) for choked flow and assuming constant temperature, the output flow depends linearly on the average spool position and supply pressure. Consequently, with a constant supply pressure, the flow percentage (ratio of flow to the maximum flow corresponding to 100% duty cycle) is equal to the percentage of the average spool position. Since experimental measurement of the averaged spool position is impossible, the measured flow data are used for comparison with the simulated data of the averaged spool position. In Fig. 10, percent of the measured flow is compared to simulated average of the spool position. The proper agreement between the two curves approves the validity of the modeling.

6. Conclusion

In this Note a nonlinear dynamical model of a pneumatic fast switching valve is developed and validated by experimental measurements. This model successfully predicts the valve characteristics and can be used as a powerful computational and simulation tool. For practical application of the model in the design of servo-pneumatic systems, a simplification strategy is proposed in which the average of spool position is calculated and used as the control

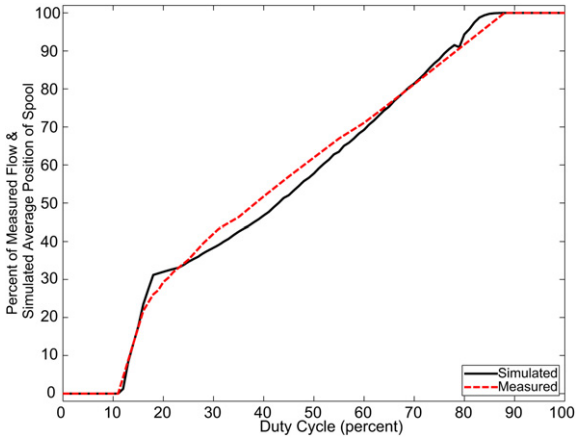

Fig. 10. Measured flow and simulated average position of spool vs. duty cycle.

variable. It is shown that the transient behavior of the average spool position is very rapid and can be neglected. As a result, the valve model between the duty cycle input and the average spool position is represented by a nonlinear static curve corresponding to a given PWM frequency and supply pressure. Finally, this static model is validated again by measuring the steady state flow of the valve.

References

[1] S.R. Goldstein, H. Richardson, A differential pulse-width modulated pneumatic servo utilizing floating flapper disc switching valves, ASME Trans. J. Basic Eng. C 143 (1968) 427–437.
[2] T. Noritsugu, Development of PWM mode electro-pneumatic servomechanism, Part I: Speed control of a pneumatic system, J. Fluid Control 17 (1) (1987) 65–79.
[3] T. Noritsugu, Development of PWM mode electro-pneumatic servomechanism, Part II: Position control of a pneumatic system, J. Fluid Control 17 (2) (1987) 7–28.
[4] X. Shen, Exploiting natural characteristics of pneumatic servo actuation through multi-input control, Ph.D. Thesis, Vanderbilt University, USA, 2006.
[5] J. Mack, ABS-TCS-VDC Where Will the Technology Lead Us? Society of Automotive Engineers, PA, USA, ISBN 1-56091-750-4, 1996.
[6] M. Sorli, S. Pastorelli, Performance of a pneumatic force controlling servosystem: Influence of valves conductance, Robot. Autonomous Syst. 30 (2000) 283–300.
[7] P. Scarfe, E. Lindsay, Air muscle actuated low cost humanoid hand, Int. J. Adv. Robot. Syst. 3 (2006) 139–146.
[8] B.L. Shields, K.B. Fite, M. Goldfarb, Design, control, and energetic characterization of a solenoid-injected monopropellant-powered actuator, IEEE/ASME Trans. Mechatronics 11 (2006) 477–487.
[9] R.B. Van Varseveld, G.M. Bone, Accurate position control of a pneumatic actuator using on/off solenoid valves, IEEE/ASME Trans. Mechatronics 2 (1997) 195–204.
[10] G. Belforte, S. Mauro, G. Mattiazzo, A method for increasing the dynamic performance of pneumatic servo systems with digital valves, Mechatronics 14 (2004) 1105–1120.
[11] T. Nguyen, J. Leavitt, F. Jabbari, J.E. Bobrow, Accurate sliding-mode control of pneumatic systems using low-cost solenoid valves, IEEE/ASME Trans. Mechatronics 12 (2007) 216–219.
[12] H.S. Jeong, H.E. Kim, Experimental based analysis of the pressure control characteristics of an oil hydraulic three-way on/off solenoid valve controlled by PWM signal, ASME Trans. J. Dyn. Syst. Meas. Control 124 (2002) 196–205.
[13] O. Keles, U. Ercan, Theoretical and experimental investigation of a pulse-width modulated digital hydraulic position control system, Control Eng. Practice 10 (2002) 645–654.
[14] J. Pohl, M. Sethson, P. Krus, J.O. Palmberg, Modeling and validation of a fast switching valve intended for combustion engine valve trains, Proc. Inst. Mech. Eng. Part I: J. Syst. Control Eng. 216 (2002) 105–116.
[15] C. Kunt, R. Singh, A linear time varying model for on–off valve controlled pneumatic actuators, ASME Trans. J. Dyn. Syst. Meas. Control 112 (1990) 740–747.
[16] E.J. Barth, J. Zhang, M. Goldfarb, Control design for relative stability in a PWM-controlled pneumatic system, ASME Trans. J. Dyn. Syst. Meas. Control 125 (2003) 504–508.
[17] A. Messina, N.I. Giannoccaro, A. Gentile, Experimenting and modeling the dynamics of pneumatic actuators controlled by pulse width modulated (PWM) technique, Mechatronics 15 (2005) 859–881.
[18] X. Shen, J. Zhang, E.J. Barth, M. Goldfarb, Nonlinear model-based control of pulse width modulated pneumatic servo systems, ASME J. Dyn. Syst. Meas. Control 128 (2006) 663–669.

[19] G.M. Bone, N. Shu, Experimental comparison of position tracking control algorithms for pneumatic cylinder actuators, IEEE/ASME Trans. Mechatronics 12 (2007) 557–561.
[20] M. Taghizadeh, A. Ghaffari, F. Najafi, A linearization approach in control of PWM-driven servo-pneumatic systems, in: Proc. 40th IEEE/SSST Sym., New Orleans, LA, USA, 2008, pp. 395–399.
[21] N. Ye, S. Scavarda, M. Betemps, A. Jutard, Models of a pneumatic PWM solenoid valve for engineering applications, ASME Trans. J. Dyn. Syst. Meas. Control 114 (1992) 680–688.
[22] E.E. Topcu, I. Yuksel, Z. Kamis, Development of electro-pneumatic fast switching valve and investigation of its characteristics, Mechatronics 16 (2006) 365–378.
[23] V. Szente, J. Vad, Computational and experimental investigation on solenoid valve dynamics, in: Proc. IEEE/ASME Int. Conf. Advanced Intelligent Mechatronics, Como, Italy, 2001, pp. 618–623.
[24] V. Zoppig, K. Feindt, T. Strohla, E. Kallenbach, Fast acting switching valves for servo-pneumatics, in: Proc. IEEE/ASME Int. Conf. Advanced Intelligent Mechatronics, 2003, pp. 302–307.